Published in final edited form as:
Dev Dyn. 2010 November ; 239(11): 2813–2827. doi:10.1002/dvdy.22418.

Drosophila *variable nurse cells* encodes Arrest defective 1 (ARD1), the catalytic subunit of the major N-terminal acetyltransferase complex

Ying Wang[1], **Michelle Mijares**[1,2], **Megan D. Gall**[1,3], **Tolga Turan**[1,4], **Anna Javier**[1], **Douglas J Bornemann**[1], **Kevin Manage**[5], and **Rahul Warrior**[1,6]

[1]Department of Developmental and Cell Biology, University of California Irvine, Irvine, CA 92697

[2] Kaiser Permanente, Los Angeles, CA.

[6]Developmental Biology Center, University of California Irvine, Irvine, CA 92697

Abstract

Mutations in the *Drosophila variable nurse cells* (*vnc*) gene result in female sterility and oogenesis defects, including egg chambers with too many or too few nurse cells. We show that *vnc* corresponds to *Arrest Defective1* (*Ard1*) and encodes the catalytic subunit of NatA, the major N-terminal acetyl-transferase complex. While N-terminal acetylation is one of the most prevalent covalent protein modifications in eukaryotes, analysis of its role in development has been challenging since mutants that compromise NatA activity have not been described in any multicellular animal. Our data show that reduced ARD1 levels result in pleiotropic oogenesis defects including abnormal cyst encapsulation, desynchronized cystocyte division, disrupted nurse cell chromosome dispersion and abnormal chorion patterning, consistent with the wide range of predicted NatA substrates. Further we find that loss of *Ard1* affects cell survival/proliferation and is lethal for the animal, providing the first demonstration that this modification is essential in higher eukaryotes.

Keywords

Drosophila oogenesis; protein N-terminal acetylation; NatA; ARD1; *variable nurse cells (vnc)*

INTRODUCTION

During Drosophila oogenesis, oocytes are generated through a tightly regulated series of cell divisions. First, germline stem cells (GSCs) in the germarium divide asymmetrically to give rise to a new GSC and a cystoblast. The cystoblast then undergoes four successive rounds of synchronous divisions with incomplete cytokinesis to form a cyst of 16 cells (cystocytes) that remain connected by intercellular bridges termed ring canals (RC). Each cyst contains eight cells with one RC, four with two RCs, and two each with three and four RCs. One of the cells with four RCs becomes specified as the oocyte, while the remaining fifteen adopt a

* Author for correspondence **Corresponding Author:** Rahul Warrior Dept of Developmental and Cell Biology 4219 McGaugh Hall, Zot 2300 University of California, Irvine Irvine CA 92697-2700 Office: (949) 824-9798. Lab: (949) 824-2597. Fax: (949) 824-4709. rwarrior@uci.edu.
[3]Current address: Department of Biological Sciences, Purdue University, Lafayette IN 47907. mgall@purdue.edu
[4]Current address: Department of Pathology, University of California Irvine, Irvine CA 92697. tturan@uci.edu
[5]Current address: Department of Biochemistry, University of California Riverside, Riverside, CA 92521. kmanage2@gmail.com mchllmijares@gmail.com

nurse cell fate. The cyst progresses posteriorly through the germarium as it matures, and in region 2a is surrounded by somatically derived follicle cells, to produce an egg chamber (reviewed in King, 1970; Mahowald and Kambysellis, 1980; Spradling, 1993). Formation of the sixteen-cell cyst requires both control of the number of cystocyte cell divisions and coordination of their synchrony. Consistent with this, several mutations that affect the activity of key cell cycle regulators have been shown to result in egg chambers with abnormal nurse cell numbers. For example, elevated levels of CyclinA (CYC A) and CyclinE (CYC E) are seen in *encore* (*enc*) females that produce egg chambers with thirty-one nurse cells and a single oocyte (Hawkins et al., 1996; Ohlmeyer and Schupbach, 2003). Extra nurse cells also result when CYC A or CYC E levels are increased by direct overexpression (Lilly and Spradling, 1996; Lilly et al., 2000) or by mutations that affect the ubiquitin-dependent cyclin degradation pathway (Ohlmeyer and Schupbach, 2003), as well as in mutants for *twin*, a CCR4 deadenylase that reduces *CycA* transcript stability (Morris et al., 2005). Hypomorphic mutations in *half pint*, a splicing factor that physically interacts with ENC have the opposite effect and result in egg chambers with eight rather than sixteen germline cells (Van Buskirk and Schupbach, 2002). Coordination of cystocyte divisions is dependent on the fusome, a large spectrin-rich membranous structure that connects all cells in a cyst through the ring canals (reviewed in Huynh, 2006). The fusome arises from the spectrosome, a spherical structure that the cystoblast inherits from the GSC. During cystocyte divisions, the spectrosome fuses with residual mitotic spindle material and assumes a branched configuration that extends through ring canals into each cell within the cyst (Yue and Spradling, 1992; de Cuevas et al., 1997; Deng and Lin, 1997; McGrail and Hays, 1997). The fusome functions as a communication channel between cells that facilitates synchronized divisions, germline cyst differentiation and oocyte specification. Mutations that disrupt structural components of the fusome, such as *α-spectrin* and the adducin homolog *hu-li tai shao* (*hts)*, result in cysts that contain reduced numbers of germline cells and lack a specified oocyte (Yue and Spradling, 1992; Lin et al., 1994; McGrail and Hays, 1997; de Cuevas and Spradling, 1998).

In addition to specialized mitoses, germline cells also display distinctive chromosomal conformations during different stages of oogenesis. Following cyst formation, the oocyte initiates meiosis and arrests in meiotic prophase I, and its chromosomes form a condensed, transcriptionally inactive karyosome. In contrast, nurse cell chromosomes go through multiple endocycles, in which DNA is replicated without accompanying cell division (King, 1970; Spradling, 1993). During these endocycles, nurse cell chromosomes undergo a major morphological change initiated during early endocycle 5. Before this stage, homologous chromosomes are aligned, and display a polytene morphology with visible banding patterns. During endocycle 5, homolog pairing weakens and the chromosomes lose their banding patterns and assume a characteristic “five-blob” structure. This morphology is transient and by the end of endocycle 5, chromosome alignment breaks down and individual chromosome pairs become uniformly dispersed throughout the nucleus (King, 1970; Hammond and Laird, 1985; Dej and Spradling, 1999). Chromosomal dispersion is thought to arise through initiation of a truncated mitotic cycle that interrupts DNA replication and allows separation of all chromosomal arms except those with unresolved replication forks. The significance of nurse cell chromosome dispersion is not clear but has been postulated to facilitate rapid ribosome synthesis (Spradling, 1993; Dej and Spradling, 1999).

Post-translational modifications play important roles in many developmental processes by affecting protein stability or activity. N-terminal acetylation is one of the most common covalent modifications in eukaryotes, occurring on approximately 80-90% of mammalian cytosolic proteins and 50% of proteins in yeast (Polevoda and Sherman, 2003b). During eukaryotic translation, the initiator methionine residue is removed from the nascent polypeptide by methionine amino peptidases. The newly exposed N-terminal residue is then

modified on its alpha-amino group by transfer of an acetyl group from acetyl-CoA while the polypeptide chain is between 25 to 50 residues long. This modification neutralizes positive a charge on the protein and is thought to influence protein function, stability and interactions with other proteins as well as subsequent modifications. Five N-terminal acetyltransferases complexes (NatA through NatE) have been identified that are conserved from fungi to humans. Among them, NatA has the most targets, with more than 2500 in yeast. NatA consists of two subunits – the ARD1/Naa10p catalytic subunit and Nat1p/Naa15p an accessory subunit that enables binding to the ribosome (reviewed in Polevoda and Sherman, 2003a; Polevoda and Sherman, 2003b). Yeast mutants lacking NatA activity are viable but exhibit a wide range of defects including slower growth, temperature sensitivity, salt sensitivity, defects in sporulation and derepression of the silent mating type gene *HMLα* (Mullen et al., 1989; Park and Szostak, 1992) In vertebrate tissue culture, knockdown of NatA subunits affects cell cycle regulation, reduces cell proliferation and induces apoptosis (Arnesen et al., 2006; Lim et al., 2006). Based on these findings and the elevated expression of NatA subunits in several human tumors, NatA has been identified as a potential cancer drug target (Arnesen et al., 2008). Other studies have suggested that NatA activity may suppress tumor growth rather than promote it, at least in the context of mTOR-dependent tumorigenesis (Kuo and Hung, 2010; Kuo et al., 2010). Despite burgeoning interest, the developmental role of NatA and its contribution to organismal function have not been addressed and mutants that affect the catalytic activity of the complex have yet to be identified in any multicellular organism.

In this paper we report the identification of null and loss-of-function mutations in *Ard1*, the catalytic subunit of *Drosophila* NatA. We show that *Ard1* corresponds to *variable nurse cells* (*vnc*) a locus identified in genetic screens for female sterile mutations (Rees, 1990; Matthews et al., 1993). Homozygous *vnc* females produce egg chambers with too many nurse cells as well as egg chambers with too few nurse cells, a phenotype that resembles the loss of germline cells seen in mutants that disrupt the Dynein/LIS-1 pathway (McGrail and Hays, 1997; Liu et al., 1999; Swan et al., 1999; Lei and Warrior, 2000). We find that *vnc* mutants show pleiotropic defects including abnormalities in fusome structure and loss of synchrony in cystocyte mitoses that are consistent with the variable nurse cell phenotypes. In addition, *vnc* mutants display defects in cyst packaging, nurse cell chromosome dispersion and the development of chorionic appendages. Our analysis reveals that *vnc* mutations are tissue-specific hypomorphic loss-of-function mutations that specifically affect *Ard1* expression in the ovary. We show that *Ard1* null mutations are lethal, demonstrating that ARD1 activity is essential for viability in a higher eukaryote.

RESULTS

Identification of a lethal *vnc* allele

The *vnc* locus was first identified by Rees and co-workers in the course of an X-ray mutagenesis screen for female sterile mutations mapping to the 67A-D genomic interval (Rees, 1990; Matthews et al., 1993). A total of 15 hypomorphic alleles were isolated, of which only two, vnc^{2} and vnc^{14}, are still extant. While *vnc* mutant males were viable and fertile, homozygous females were reported to have egg chambers with abnormal numbers of nurse cells (Rees, 1990). Based on the predicted map position and partial phenotypic overlap with dynein pathway mutants, *vnc* alleles were potential candidates for mutations in the *nudE* gene that encodes a component of the LIS-1/cytoplasmic dynein motor complex (Kardon and Vale, 2009). To more precisely map the *vnc* locus, we tested all available lethal or sterile mutations in the 67A2-D14 region and determined if any failed to complement the fertility defects in *vnc* mutants. We found that only *l(3)67BDk*, one of 23 previously reported lethal loci identified in ethyl methanesulfonate and diepoxybutane-based mutant screens of the 67B-D region (Leicht and Bonner, 1988), was female sterile in *trans* to both

vnc alleles. These results as well as molecular analyses (see below) indicated that *l(3)67BDk* corresponds to a lethal mutation in *vnc*, henceforth refered to as vnc^{BDk}. Identification of this lethal allele simplified molecular mapping and characterization of the gene.

Egg chamber formation is affected in *vnc* mutants

To control for potential background mutations, we examined females transheterozygous for the independently isolated vnc^{BDk} and vnc^{14} alleles, as well as vnc^{14} homozygotes. Females with both genotypes produce fewer eggs than wild type, the majority of which are shortened along the anterior/posterior axis and collapsed. In addition eggs laid by *vnc* mutant females frequently (24.6% for vnc^{14}/vnc^{14}; 28.2% for vnc^{14}/vnc^{BDk}) show defects in the shape or position of the dorsal appendages (DAs), such as appendages that are closely apposed or fused (Fig. 1A-C and Table 1, row 8) suggestive of ventralization. In a few cases we observed eggs with supernumerary DAs (Fig. 1D). Examination of dissected ovaries revealed several additional defects. Oocyte growth in *vnc* mutants appears essentially normal until stage 10 when the oocyte occupies 50% of the volume of the egg chamber. However many egg chambers (44.4% vnc^{14}/vnc^{14}; 38.5% vnc^{14}/vnc^{BDk}) that appeared to be at stage 11 or older based on follicle cell morphology, contained unusually small oocytes and persistent nurse cells (Fig. 1E; Table 1, row 7), phenotypes that typically result from a failure of nurse cells to transfer or dump their contents into the oocyte at stage 11 (Cooley and Theurkauf, 1994).

Wild-type egg chambers contain 15 nurse cells and an oocyte surrounded by a layer of somatically derived follicle cells (Fig. 1F). In contrast, the number of nurse cells in ovaries from *vnc* females varied widely from 1 to more than 60 (Fig. 1G, H). Visualization of nurse cell nuclei by staining with the DNA dye DAPI revealed that 50% of vnc^{14} and 13.3% of vnc^{14}/vnc^{BDk} mutant egg chambers contained abnormal numbers of germline cells (Table 1, rows 4 and 5 summed). The diverse morphological defects observed suggest that *vnc* activity has important and pleiotropic roles in egg chamber formation.

vnc ovaries have defects in follicle cell encapsulation and cystocyte mitoses

Defects in at least two distinct processes are known to give rise to egg chambers with excess germline cells. First, instead of surrounding a single 16-cell cyst, follicle cells in mutant ovaries can encapsulate several cysts or partial cysts. Compound egg chambers generated through this process include additional nurse cells and oocytes derived from independent cysts that have undergone no more than four divisions, and therefore all cells have four or fewer ring canals. Further, since misincorporated germline cells in compound egg chambers may have more than one ring canal, the number of ring canals may exceed the number of nurse cell nuclei. Egg chambers with excess germline cells can also be formed when germline cells undergo additional rounds of mitosis. If the extra division occurs in a cystocyte that already has four ring canals, one of the daughter cells will have five ring canals. Since each germline division produces both an extra cystocyte and an additional ring canal that marks the position of incomplete cytokinesis, these extra divisions generate cysts containing equal numbers of nurse cells and ring canals.

To determine whether egg chambers with extra nurse cells arose from one or both of these processes, we co-stained ovaries from vnc^{14} homozygotes with antisera against HTS-RC that specifically stains ring canals and against ORB which accumulates in specified oocytes (Lantz et al., 1994; Huynh and St Johnston, 2000). In 26.4% of vnc^{14} and a lower fraction (8.2%) of vnc^{14}/vnc^{BDk} egg chambers we observed several foci of ORB staining, indicating the presence of multiple specified oocytes (Table 1, row 5). Analysis of HTS-RC staining showed that each of these oocytes was associated with no more than four ring canals, suggesting they had developed in independent cysts and had been mispackaged (Fig. 2A, B).

In addition to supernumerary germline cells resulting from encapsulation defects, a significant fraction (12.3%) of abnormal *vnc*^{14} egg chambers were clearly generated through extra mitoses (Table 1, row 4 and legend). For example, the egg chamber in Fig. 2C has 30 nurse cells and a single oocyte that is positioned normally at the posterior. The oocyte is associated with 5 ring canals consistent with it having undergone an extra round of cell division. However, a total of only 30 ring canals are present rather than the 31 expected if all germline cells had undergone an extra round of division. This suggests that an extra division occurred in all but one germline cell. Thus unlike normal cystocyte divisions, the extra divisions were not perfectly coordinated for all cells within the cyst. In other egg chambers only a few additional germline cells were present. For example, the egg chamber in Fig. 2D contains 16 nurse cells and 16 ring canals rather than 15 of each, consistent with only one germline cell within the cysts having undergone an extra division. Importantly, only four ring canals are present on the oocyte, indicating that it did not undergo an additional cell division. We also observed occasional egg chambers with binucleate oocytes (Fig. 2E, F). Some of these contained varying numbers of additional nurse cells (Fig. 2E) underscoring the fact that mitosis appears to be desynchronized in *vnc* mutants; while others contained the normal number of nurse cells suggesting that only the oocyte had undergone an additional asynchronous division unaccompanied by cytokinesis (Fig. 2F). The occurrence of binucleate oocytes could explain the presence of supernumerary DAs in eggs laid by *vnc* mutant mothers (see Fig. 1D).

In contrast to the extra-nurse-cell phenotype, 11.3% of *vnc*^{14} egg chambers contained fewer germline cells than wild type (Table 1, row 4 and legend). These egg chambers usually had equal numbers of ring canals and nurse cells suggesting an underlying failure of one or more germline cystocyte cells to divide, rather than encapsulation defects. For example, 7 nurse cells, 7 ring canals and a single oocyte are present in the egg chamber in Fig. 2G compatible with a failure of all cells in the cyst to complete the last division. In other instances egg chambers lack one or more nurse cells, consistent with a failure of individual germ line cells to divide (Fig 2H). Thus it appears that the variable-nurse-cell-number phenotype results from both aberrant cyst encapsulation by follicle cells, and too many or too few cystocyte divisions.

vnc mutants display altered fusome morphology

Since impaired fusome function can lead to failure of cystocyte division synchrony, abnormal cyst formation and variable cystocyte number (McGrail and Hays, 1997; Liu et al., 1999; Mathe et al., 2003), we examined fusome morphology in ovarioles stained with anti-Adducin antisera 1B1 (Zaccai and Lipshitz, 1996). Wild type cysts contain intact, smoothly branched fusomes (Fig. 3A). In *vnc* mutant cysts several defects were observed, including a reduction in the amount of fusome material (Fig. 3B-E′). In addition, the morphology of the fusome was altered. Mutant cysts often contained thinner and fragmented fusomes (Fig. 3B, B′). Some cysts contained large spherical or barbell shaped fusomes (Fig. 3C-D′), a phenotype frequently observed when cystoblasts fail to divide (McGrail and Hays, 1997; Liu et al., 1999; Mathe et al., 2003). In severe examples mutant *vnc* germaria can be seen that contain a few spherical fusomes and cysts with reduced germline cells (Fig. 3D, D′). Finally, in some *vnc* germaria fusomes persist as late as region 3 (Fig. 3E, E′). This is in contrast to wild type where fusomes disassemble and are no longer visible by the middle of region 2a (see Fig. 3A, A′; Lin et al., 1994). In sum, fusome defects were seen in 46.7% of *vnc*^{14} and 28.3% of *vnc*^{14}/*vnc*^{BDk} germaria (Table 1, row 1). Consistent with the presence of some 15-nurse-cell egg chambers at later stages, we also observed cysts with apparently normal fusomes (data not shown).

In addition to enabling the coordination of cystocyte divisions, fusomes are also important for oocyte specification (Lin and Spradling, 1995). In wild type ovaries, the cystocyte that

retains the most fusome material is specified as the oocyte (Lin et al., 1994; de Cuevas and Spradling, 1998), while mutants with disrupted fusome morphology often fail to specify or misspecify oocytes (McKearin and Ohlstein, 1995; McGrail and Hays, 1997; McKearin, 1997; Liu et al., 1999). To test whether alterations in *vnc* activity affect oocyte specification, we stained germaria with antisera against the oocyte-specific molecular markers ORB, Egalitarian (EGL) and C(3)G. In wild type the RNA binding protein ORB is initially expressed in all cystocytes, but is subsequently restricted to just two pro-oocytes by germarial region 2a and further refined to the oocyte by region 2b (Fig. 4A; Lantz et al., 1994). ORB localization appeared normal in the majority of cases although in 10.5% of vnc^{14} and 11.4% of vnc^{14}/vnc^{BDk} germaria, staining was greatly reduced or absent in region 1-2a (Fig. 4B; Table 1 row 3). A similar loss of staining was also observed for EGL, another early cystocyte marker whose expression is progressively restricted to the oocyte by region 2b (data not shown). Despite the lack of ORB staining in a subset of early ovarioles, oocyte-specific ORB staining was generally detectable in all egg chambers after stage 2 (Fig. 4B). This result suggests that the restriction of ORB and EGL to the oocyte may be delayed in a subset of *vnc* cysts or that these cysts fail to mature.

Staining for C(3)G, a synaptonemal complex (SC) component (Page and Hawley, 2001) yielded similar results. Formation of the SC, a precursor to meiosis, initially occurs in two to four cells per cyst in region 2a (Fig. 4C). However only the specified oocyte retains the SC through later stages and eventually completes meiosis (Fig. 4C). We found that in *vnc* ovaries C(3)G staining was unaffected in the majority of germaria. However in a subset of ovarioles progressive restriction of the SC into a single cell was delayed, and C(3)G staining could be seen in up to four cells as late as germarial stage 3 (Fig. 4D). In other mutant cysts C(3)G staining was entirely absent after region 2a, suggesting failure to maintain the SC in the oocyte (Fig. 4E). In total, aberrant C(3)G localization was detected in 12.8% and 13.2% of germaria from vnc^{14} and vnc^{14}/vnc^{BDk} females respectively (Table 1, row 2). The presence of both persistent expression and loss of C(3)G staining in *vnc* mutants could be due to improper distribution of oocyte-determining components: cystocytes that aberrantly receive determinants above a critical threshold would fail to restrict the SC, while oocytes with below-threshold levels of these components would fail to maintain it. We conclude that the wide spectrum of fusome defects in *vnc* mutants are likely to contribute to the aberrant germline cell number observed in *vnc* mutant egg chambers through effects on the synchrony of cystocyte divisions.

Mutations in *vnc* affect chromatin reorganization in nurse cell nuclei

During oogenesis, nurse cell chromosomes undergo stereotypic conformational changes tightly correlated with the endocycle (Dej and Spradling, 1999). For the first four endocycles homologous chromosomes are joined together and nurse cell chromatin displays a polytene-like banded appearance. In endocycle 5, homolog pairing weakens and chromosomes assume a “five-blob” conformation, in which each individual chromosome arm is still distinguishable (Fig. 5A, S5 inset). At the end of this endocycle, the blob-like chromatin masses decondense and chromosomes become evenly dispersed as individual chromatid pairs throughout the nucleus (Fig. 5A, S6 inset). In vnc^{14} mutant egg chambers this dispersal process is severely disrupted with 70.3% of the nurse cells beyond stage 5 retaining the five-blob conformation (Fig 5B). In contrast, only 3.2% of wild type nurse cell nuclei display this organization beyond stage 5 (Table 1, row 6). A similar penetrance is observed in vnc^{14}/vnc^{BDk} heteroallelic egg chambers (72.8%). The condensed five-blob chromosome conformation can persist in *vnc* mutant egg chambers beyond stage 10 (Fig. 5C). The dispersion of nurse-cell chromatin during endocycle 5 is thought to result from entry of the polyploid nurse cell nuclei into a truncated mitotic phase that begins before completion of chromosome replication (Dej and Spradling, 1999). By contrast, nurse cell nuclei prior to

endocycle 5 undergo complete rounds of S-phase replication without entering M phase. The persistence of the five-blob conformation in *vnc* mutants suggests that entry into the truncated mitotic phase may be blocked, allowing completion of S-phase replication and retention of the 5-blob chromatin conformation without dispersion well beyond S5 (Fig. 5C). Thus, while *vnc* activity does not appear to affect S-phase DNA replication, it may impact entry into the early stages of mitosis.

vnc activity is required for somatic cell growth and division

To investigate whether there is a broader requirement for *vnc* in other stages of development, we examined the phenotypes of homozygous vnc^{BDk} animals. Homozygotes for vnc^{BDk} perish during the second larval instar, similar to hemizygotes in *trans* to a small deficiency $Df(3L)vnc^{MK}$ (see below). The comparable lethal phases argue that vnc^{BDk} likely represents a strong loss-of-function or null allele. We were unable to determine the contribution of maternally provided *vnc* RNA and protein to embryonic development since the few eggs laid by vnc^{2} and vnc^{14} homozygotes are unfertilized and germline clones mutant for the vnc^{BDk} allele could not be recovered. To examine the requirement for *vnc* activity in larval tissues we used FRT mediated recombination to generate clones of mutant cells in wing imaginal discs. Late induction of mitotic recombination yielded small clones homozygous for vnc^{BDk} that were marked by the absence of GFP (Fig. 6, asterisks), paired with significantly larger twin spots of homozygous wildtype cells. Clones induced at earlier stages gave rise to large wild type twinspots, without any accompanying mutant clones (Fig. 6, arrows). The inability to recover large mutant clones suggests that *vnc* activity is required for cell proliferation or survival.

vnc encodes ARD1, the catalytic subunit of an N-terminal acetyltransferase

As a first step towards determining the molecular identity of *vnc*, we used high-resolution meiotic mapping to determine the gene location relative to P-element transposons with molecularly defined insertion points (Zhai et al., 2003). We obtained five Pw^{+} transposons inserted in the 67A-D region (Fig. 7A). Each stock was individually crossed to vnc^{BDk} to produce daughters in which meiotic recombination between the P-element and vnc^{BDk} could occur. These females were crossed to hemizygotes for *Df(3L)AC1*, a deficiency that fails to complement *vnc*, balanced with a temperature-sensitive lethal third chromosome balancer. Progeny were raised under restrictive conditions to eliminate balancer animals. As a result, only two classes of viable progeny were possible: red-eyed non-recombinants carrying the P-element and white-eyed recombinants lacking the P-element (see Materials and Methods; Zhai et al., 2003). By scoring ~ 5000 progeny per cross we were able to determine the map distance between each P-element and vnc^{BDk} with a resolution of approximately 0.1 cM. These data indicated that vnc^{BDk} is approximately 0.05 cM or 55 kb distant from the closest P-element, $P\{SUPor\text{-}P\}dpr6^{KG07985}$, inserted in the first intron of the *defective proboscis response 6 (dpr6)* gene (Fig. 7A).

To further refine the location of *vnc*, we mobilized this P-element and screened for small deletions generated through imprecise excision. Complementation analysis with vnc^{BDk} yielded two lines, vnc^{M2} and vnc^{MK} that failed to complement the sterility defect of vnc^{2}. The extent of the lesions caused by the imprecise excisions was determined using PCR. We found that both excision alleles contained deletions that extended distally from the P-element insertion site. The deletion vnc^{MK} extended 4 kb upstream of *dpr6* and disrupted five genes: *dpr6*, *CG6685*, *Nc*, *CG6674* and *Ard1*, identifying them as candidate open reading frames for *vnc*. Sequencing of genomic DNA isolated from vnc^{2}, vnc^{14} and vnc^{BDk} homozygous embryos or adults in the region of candidate genes revealed molecular lesions in the *Ard1* gene in all three cases. Both vnc^{2} and vnc^{14} animals contain a 5.2 kb copia element inserted at an identical location in the only predicted intron of *Ard1* (Fig. 7A), while

in vnc^{BDk} the *Ard1* coding region is interrupted by a 20 bp deletion and 14 bp of novel sequence generating a truncated protein predicted to lack the entire ARD1 C-terminal region as well as a portion of the acetyltransferase domain (Fig. 7A-C). Consistent with *vnc* corresponding to *Ard1*, vnc^{BDk} failed to complement P{EPgy2}$Ard1^{EY23147}$, a lethal mutation linked to a P-element inserted 5′to the *Ard1* open reading frame.

The *Ard1* locus is predicted to encode the *Drosophila* ortholog of human ARD1a (also referred to as Naa10p), the catalytic subunit of NatA, a highly conserved N-terminal acetyltransferase (Polevoda et al., 2009). In yeast and humans, the NatA complex, consisting of ARD1 and an auxiliary subunit Nat1/Naa15p, is anchored to ribosomes and acetylates nascent peptides (Gautschi et al., 2003). ARD1 proteins show extensive sequence conservation and the *Drosophila* homolog shares 69.6% and 47.1% identical residues with human ARD1a and yeast ARD1 respectively (Fig. 7B, C). Like other acetyltransferase catalytic subunits, ARD1 contains an acetyltransferase enzymatic domain (residues 52-139) that harbors an acetyl-CoA binding site (RRLGLA; (Schultz and Pils, 2002). A predicted nuclear localization signal (KRSYRR; (Chelsky et al., 1989) is also present within the acetyltransferase domain.

To confirm that the *vnc* phenotypes are indeed caused by lesions in *Ard1*, we generated a genomic rescue construct containing the *Ard1* coding region and 1.3 kb of flanking sequences (see Fig. 7A). This transgene successfully restored vnc^{14} and vnc^{14}/vnc^{BDk} mutants to full viability and fertility. Analysis of eggs and egg chambers revealed that in the presence of the transgene the frequency of all oogenesis defects assayed was reduced to near wild type levels (Fig. 5C, D; Table 1), unambiguously demonstrating that the *vnc* locus corresponds to the *Ard1* gene.

Since the copia insertion in vnc^{2} *and* vnc^{14} is in the *Ard1* intron and does not alter the protein sequence, we hypothesized that the lesion might affect *Ard1* expression in the ovary. To examine ARD1 levels in *vnc* mutants, we first determined whether polyclonal antisera against human ARD1 could recognize the homologous fly protein. Total protein extracts from wild type and *vnc* allelic combinations were separated on SDS poly-acrylamide gels, transferred to nitrocellulose filters, and the western blots probed with anti-human ARD1. A single band running at ~22 kDa was detected in larval extracts from wildtype and $Df(3L)vnc^{MK}$/+ hemizygotes consistent with the 22.3 kDa molecular weight of the conceptually translated protein (Fig. 7D left panel, lanes 1 and 3). No signal was seen in $vnc^{BDk}/Df(3L)vnc^{MK}$ mutant extracts (Fig. 7D left panel, middle lane). The presence of a single appropriately sized band in wild type and its absence from mutant extracts argues that the antisera specifically recognize *Drosophila* ARD1. The failure to detect the truncated 17 kDa polypeptide encoded by vnc^{BDk} allele could be due to the absence of critical antigenic epitopes or because of instability of the mutant protein, consistent with the strong loss-of-function phenotype. Comparison of ARD1 expression levels in ovaries from wild type and a hypomorphic *vnc* mutant revealed that ARD1 levels in vnc^{BDk}/vnc^{14} and vnc^{14}/vnc^{14} ovaries are indeed dramatically decreased compared to wild type controls (Fig. 7D, right panel).

Microarray data and RNA-seq analysis from the modENCODE project indicate that *Drosophila Ard1* is widely transcribed (Chintapalli et al., 2007) and the NatA complex is predicted to be active in most tissues. Therefore the fact that phenotypic defects in vnc^{2} and vnc^{14} mutants were restricted to oogeneisis could reflect a more stringent requirement for N-terminal acetylation during oogenesis, or alternatively, result from a specific reduction in *Ard1* levels or activity in ovaries. To distinguish between these possibilities we used quantitative PCR to compare *Ard1* mRNA levels in ovaries and other tissues from wild type and *vnc* mutant adults. We found that *Ard1* transcript levels in mutant ovaries decreased, while *Ard1* transcripts in other tissues were marginally increased. In fact, a four-fold

reduction in transcript levels was seen in ovaries from vnc^{14} homozygotes mutant and an eight-fold decrease in vnc^{14}/vnc^{BDk} ovaries (Fig. 7E). At the same time we observed a two-fold increase for *Ard1* transcripts in vnc^{14}/vnc^{14} female carcasses and a 50 percent increase in vnc^{14}/vnc^{BDk} carcasses (Fig. 7E). Based on these results we conclude that vnc^{2} and vnc^{14} mutants are viable and male fertile but show pleiotropic phenotypes in oogenesis due to ovary-specific reduction in *Ard1* expression.

DISCUSSION

Mutations at the *vnc* locus were identified more than twenty years ago based on their female sterility and dramatic effects on oogenesis. In this study, we have identified lethal mutations in *vnc* and have shown that it encodes the *Drosophila* ortholog of ARD1, the catalytic subunit of the major N-terminal acetyltransferase complex. Although N-terminal acetylation is estimated to occur on 84% of human proteins, making it one of the most common post-translational protein modifications, its functional consequences are not well understood (Arnesen et al., 2009). Indeed, the initial lack of identified *Drosophila* targets led to speculation that this modification might be rare in invertebrates (Polevoda and Sherman, 2003b). Recent proteomic analyses showing that approximately 71% of nascent *Drosophila* cytosolic proteins undergo N-terminal acetylation contradict this idea and argue that this covalent modification is likely to have important biological functions in both invertebrates and vertebrates (Goetze et al., 2009). Given the sheer number of NatA targets and the wide range of functions they participate in, determining which proteins require N-terminal acetylation for function has proved challenging, particularly in the absence of mutations that specifically abolish N-acetyltransferase catalytic activity. Thus the identification of loss-of-function alleles in *Ard1* provides important reagents that can be used to dissect the biological functions of this evolutionarily conserved protein modification.

N-terminal acetylation is catalyzed by three major (NatA, NatB and NatC) and two minor complexes (NatD and NatE) that are conserved from yeast to humans (Polevoda et al., 2009). Of these, NatA appears to play the most prominent role, based on the number of substrates and the severity of phenotype observed in hNatA knockdowns in cell culture. The NatA complex, consisting of ARD1 and an auxiliary protein, Nat1p (Park and Szostak, 1992; Polevoda et al., 2009) has been shown to associate with ribosomes where it is thought to acetylate the N-termini of nascent polypeptides during translation (Gautschi et al., 2003). The substrate specificity of NatA is limited to proteins bearing Serine, Alanine, Glycine, Threonine, Valine and Cysteine following the start Methionine. This specificity appears to be evolutionarily conserved, since yeast lacking yARD1 and yNat1 can be rescued by simultaneously supplying both human orthologs. Proteomic analysis of this rescued strain showed that the yeast and human complexes have nearly identical target specificities (Arnesen et al., 2009). Yeast NatA has been shown to modify >2,000 proteins, and this may still be an underestimate. Both ARD1 and Nat1p are found in non-ribosome-associated as well as ribosome-associated complexes, suggesting that NatA may acetylate internal epsilon as well N-terminal amino groups (Arnesen et al., 2005). Indeed human ARD1 has been implicated in acetylation of lysine epsilon-amino groups in Hypoxia-Inducible Factor 1α (Jeong et al., 2002) and β-catenin (Lim et al., 2006), although this has not been conclusively demonstrated *in vivo*.

Our identification of vnc^{BDk} as a lethal allele of *Ard1* demonstrates that ARD1 function is required for viability, the first such demonstration in the context of a multicellular organism. A subset of *Ard1* transcripts are reported to be dicistronic and to contain an upstream open reading frame that could potentially encode a 78 residue peptide (Hayden and Bosco, 2008). The open reading frame is unaffected by vnc^{BDk} lesion. Homozygotes for vnc^{BDk} die as second-instar larvae. Their survival to this stage is likely supported by a robust wild type

maternal contribution, given our findings that homozygous mutant clones in the wing disc fail to grow beyond three cells in size, and germline clones of the lethal allele could not be recovered. The importance of *Ard1* activity for normal development and function is underscored by the multiple oogenesis defects, including aberrant mitoses, defects in egg chamber encapsulation and nurse cell chromatin dispersion that result from ovary-specific reduction in transcript levels in female-sterile alleles of *vnc*.

The variable nurse cell phenotype correlates with defects in fusome morphology

Wild type cystoblasts undergo four synchronous rounds of cell division to produce 16 cystocytes that remain cytoplasmically interconnected through ring canals and the fusome, a vesicle-rich structure that consists of modified endoplasmic reticulum (Snapp et al., 2004). The fusome endomembranes form a continuous connection through the ring canals that enables oocyte specification and cell division synchrony. Mutations in genes such as *hts* and *α-spectrin* that cause fusome disruption result in reduced numbers of cystocyte divisions, failure of division synchrony and defects in oocyte specification (Lin et al., 1994; de Cuevas et al., 1996). During mitotic divisions the cystoblast that retains the most fusome material differentiates as the oocyte (reviewed in Huynh, 2006), whereas synchrony of cystocyte divisions is mediated through coordinated degradation of fusome-associated cyclins (Lilly et al., 2000) Thus germline expression of ubiquitin-protease resistant CycA induces an extra round of cystocyte division, creating egg chambers with 32 cystocytes. Likewise, hypomorphic mutations in *UbcD1* which encodes an E2 Ubquitin conjugating enzyme, produces 32-cell cysts with highly branched fusomes.

While some ovarioles in *vnc* mutants contain normal-looking fusomes, others display a wide variety of fusomal defects, including cysts lacking fusomes, cysts with abnormally thin, threadlike fusomes, and fragmentary or spherical fusomes (see Fig. 3). Moreover, while fusomes are lost in wild type cysts by germarial region 2a, some *vnc* mutant ovarioles showed persistent fusome staining as late as region 3. These diverse fusome defects could explain the wide variety of phenotypes observed in late stage *vnc* egg chambers (see Table 1). For example, fragmentation or loss of the fusome would be expected to lead to loss of cystocyte division synchrony (Lin et al., 1994;de Cuevas et al., 1996), while abnormal persistence of the fusome beyond region 2a could contribute to the additional cystoblast divisions that give rise to the egg chambers with large numbers of germline cells.

N-terminal acetylation mutants and chromatin defects

Among the diverse phenotypes encountered in *vnc* mutants, defects in nurse cell chromatin morphology are detected with the highest penetrance (see Table 1). In wild type egg chambers polytene nurse cell chromosomes assume a 5-blob morphology at endocycle 5 that disperses by the end of the endocycle (Dej and Spradling, 1999). In *vnc* mutant nurse cells, chromosomes also adopt the 5-blob conformation by stage 5, but fail to disperse and retain the condensed morphology through subsequent endocycles (see Fig. 5). However DAPI stained nurse cell nuclei fluoresce with increased intensity in later stage egg chambers indicating that despite the failure of chromosomes to disperse, multiple subsequent rounds of replication occur. The dispersal of nurse cell chromatin after endocycle 5 shares several characteristics with entry into a normal M phase and has been suggested to constitute a pseudomitosis (Dej and Spradling, 1999). In support of this idea, *morula*, a component of the Anaphase Promoting Complex/Cyclosome (APC/C) which facilitates completion of mitosis in diploid cells, is first required in nurse cells at this stage to prevent inappropriate reversion to a full-blown mitotic state that includes chromatin condensation and spindle formation (Reed and Orr-Weaver, 1997;Kashevsky et al., 2002). The failure of chromatin dispersal in *vnc* mutant nurse cells may reflect disruption of this mitosis-like phase. This defect, coupled with continued S-phase DNA replication suggests that some aspects of the

progression into mitosis could be highly sensitive to decreased ARD1 levels. If this requirement extends to somatic cells, it would be predicted to impact cell proliferation. Consistent with this expectation, vnc^{BDk} mutant clones in wing discs failed to proliferate beyond three cells (see Fig. 6). The finding that knockdown of *Ard1* inhibits cell division in the HepG2 human liver cell line (Fisher et al., 2005) supports the idea that ARD1 plays an important role in cell proliferation.

In *Drosophila* the Naa50p/Nat5p ortholog Separation Anxiety (SAN) has been shown to co-purify with ARD1 and NatA in embryonic extracts (Williams et al., 2003). SAN is also predicted to have N-terminal acetyltransferase activity, but modifies a substrate (Met-Leu) not recognized by ARD1 (Polevoda et al., 2009). Mutations in *san* cause defects in chromosome segregation at the embryonic syncitial blastoderm stage (Pimenta-Marques et al., 2008) and in sister chromatid cohesion in *Drosphila* neuroblasts (Williams et al., 2003). The premature separation of sister chromatids in *san* mutants suggest that SAN normally promotes centromeric sister chromatid cohesion, in contrast to ARD1 that may enhance chromatid separation based on the failure of nurse cell chromosomes to disperse in *Ard1* mutants. Thus *Ard1* and *san* mutants appear to display opposite defects, albeit in distinct tissues. Since ARD1 and SAN co-purify, it is possible that their activities are linked. However, even though SAN is expressed in nurse cells (and oocytes), *san* mutant germline clones show no detectable phenotypes (Pimenta-Marques *et al.* 2008), and *vnc* phenotypes are unaffected by heterozygosity for *san* (YW and RW unpublished data) arguing against the involvement of SAN in nurse cell separation. In addition, knockdowns in *san* homologs do not affect NatA-mediated acetylation in lower eukaryotes (Gautschi et al., 2003). Conversely, although knockdown of human SAN caused chromosome cohesion defects in HeLa cells, knockdowns of Nat1p did not result in mitotic defects, suggesting that SAN can support cohesion in the absence of the rest of the NatA complex (Hou et al., 2007). The absence of oogenesis defects in Drosophila *san* mutants could be due to redundancy with some other factor in this tissue.

vnc mutants show phenotypic overlap with potential ARD1 substrates

The pleiotropic phenotype of *vnc* mutants overlaps with the phenotypes of many genes that play key roles in oogenesis. Thus mutations that affect HTS disrupt fusome organization while alterations in *CycA*, *CycB* and *CycE* activity and mutations in genes such as *enc*, *cullin 1/lin19*, *effete/ubcD1*, *ubcD2*, *twin*, *half-pint/polyU binding factor 68 (pUf68)*, *Lis-1*, *Dhc64C* and *γ-tubulin* result in cysts with too many or too few germline cells. Encapsulation defects similar to those seen in *vnc* ovarioles are found in mutants that perturb Notch and Jak-Stat signaling pathways as well as when follicle cell precursor numbers are reduced (reviewed in Horne-Badovinac and Bilder, 2005), while binucleate oocytes are also encountered in hypomorphic mutants for *spaghetti squash* (*sqh*) that encodes the myosin light chain (Roth et al., 1999). Defects in genes that affect *gurken* (*grk*) localization, translation or signaling, with consequent effects on chorionic patterning result in alterations in DA morphology and placement reminiscent of those seen in *vnc* eggs. Finally, mutations in genes such as *cup*, *ovarian tumor*, *spoon*, *Hrb27C*, *fs(2)B*, *pUf68*, *squid*, *Survival motor neuron (Smn)* and *rhino* result in defects in nurse cell chromosome dispersion similar to *vnc* alleles. Rhino encodes a germline-specific homolog of Heterochromatin Protein 1 (HP1; Volpe et al., 2001) and is required for piRNA production and transposon silencing (Klattenhoff et al., 2009) while the other loci appear to be involved in regulation of mRNA splicing or translation and interact either genetically or functionally, suggesting they may affect a common pathway (Goodrich et al., 2004; Neuman-Silberberg, 2007; Lee et al., 2009). Many of these genes encode polypeptides that are potentially direct targets for ARD1 mediated N-terminal acetylation based on their predicted sequence (Arnesen et al., 2009 and supplementary Table S1). Other genes that show phenotypic overlap with *vnc* mutants could

be affected indirectly, by reduction in ARD1 levels. The identification of *in vivo* targets for ARD1 and determining the functional consequences of this protein modification are important areas for further investigation.

EXPERIMENTAL PROCEDURES

Drosophila stocks

All fly strains were from the Bloomington Stock Center and were raised on standard media at 25°C, with constant humidity. Stocks used included *vnc*^{2} *kni*$^{ri-1}$ *e*^{1}/ *TM3 Sb*^{1}, *vnc*^{14} *kni*$^{ri-1}$ *e*^{1}/*TM3 Sb*^{1}, *l(3)67BDk*^{1} *kni*$^{ri-1}$ *p*^{p}/ *TM3 Sb*^{1}, *y*^{1} *w*^{67c23}; P{EPgy2}*Ard1*^{EY23147} and *Df(3L)AC1 rn*$^{roe-1}$ *p*^{p}/ *TM3 Sb*^{1} a deficiency for 67BD region. The P-element lines *y*^{1} *w*^{67c23}; P{SUPor-P}KG02042 *ry*^{506}, *y*^{1} *w*^{67c23}; P{SUPor-P}CG3204^{KG0312} *ry*^{506}, *y*^{1} *w*^{67c23}; P{SUPor-P}CG8177^{KG01611} *ry*^{506}, *y*^{1} *w*^{67c23}; P{SUPor-P}dpr6^{KG07985} *ry*^{506}, and *y*^{1} *w*^{67c23}; P{SUPor-P}KG03548 *ry*^{506} were used for recombination mapping.

High resolution recombination mapping

The *vnc* locus was mapped with a resolution of +/− 50 kb by determining the recombination distance (RD) between the lethal *vnc*^{BDk} allele (alternatively called *l(3)67BDk*^{1}) and five P transposon lines with molecularly defined insertion sites in the 67BD region (see above and Table 2). Virgin female *vnc*^{BDk} *kni*$^{ri-1}$ *p*^{p}/ *TM3 Sb*^{1} adults were crossed to males from each P insertion strain. The female progeny *vnc*^{BDk}/P{*w*$^{+}$} were mated to *Df(3L)AC1*/*TM3 hs-hid* males. Four day old larvae were subjected to a two hour heat shock at 37°C. The only progeny expected to eclose are red eyed P{*w*$^{+}$}/*Df(3L)AC1* and white eyed flies resulting from recombination between the P{*w*$^{+}$} insertion and *vnc*. The recombination distance (RD) in centi-Morgans was deduced by determining the percentage of white eyed progeny (Zhai et al., 2003). For each P insertion, roughly 5000 F2 offspring were scored for eye color (see Table 2). The projected molecular distance (PMD) of the *vnc*^{BDk} lesion from individual P insertions was calculated based on the known molecular position of the inserts and the recombination distance (RD) to the lesion as described (Zhai et al., 2003).

Mobilization of P element to induce imprecise excision

Imprecise excision of *dpr6*^{KG07985} a P*w*$^{+}$ transposon inserted at nucleotide 9968287, 1321 bp 3′ of the predicted *Ard1* stop codon, was used to generate two small deficiencies that delete *vnc*, *Df(3L)vnc*^{M2}/*TM3 Sb* and *Df(3L)vnc*^{MK}/*TM3 Sb*. Flies homozygous for the transposon are viable and fertile. Female P{*w*$^{+}$} flies homozygous for the insert were mated to males carrying the Δ2-3 transposase source. White eyed male progeny were selected and used to establish stocks that were tested for sterility and lethality. Heterozygous adults from lethal lines were tested for their ability to complement the fertility defects in *vnc*^{2} and *vnc*^{14} mutants. Two independent lines M2 and MK were sterile in *trans* to both *vnc*^{2} and *vnc*^{14}. PCR analysis of genomic DNA isolated from homozygous mutant embryos revealed that both lines contain small deletions extending from the insertion site that completely remove the *Ard1* locus as well as the adjacent *Nc* open reading frame. These two stocks were named *Df(3L)vnc*^{M2} and *Df(3L)vnc*^{MK}.

Molecular characterization of *vnc*

The molecular lesions in *vnc*^{2}, *vnc*^{14} and *vnc*^{BDk}, were characterized by directly sequencing PCR products generated from genomic DNA isolated from homozygous mutant animals. Primers used include: CG6685F: 5′-GGTTGGGGCATTTGGCATAG-3′; CG6685R: 5′-GCAGCGTTTATTTGACCACCAG-3′; Nedd2F: 5′-CGCTCGTTGGTCCTTTTGTTTC-3′; Nedd2R: 5′-CGGGAATGATTTCGTTTATCGC-3′; CG6674F: 5′-TTTGGCTTATGCGGCTTTTG-3′; CG6674R: 5′-TTACCAGGTGACAGACCATCC-3′;

Ard1 Cloning F: 5′-CACCCGTTTGGCTGAAAATTCCTGC-3′; Ard1 Cloning R2: 5′-CATCAATAAAGTATGTTTACCGTTGGA-3′; Ard1 RT PCR1726F: 5′-CTTAGTGTGGAAGAAGTGTGC-3′; Ard1ORFF1: 5′-AATCAACAGCCACACCACCACG-3′; Ard1ORFF2: 5′-TAGCGGTCAAGCGTTCCTATCG-3′; Ard1ORFR2: 5′-TTGGTGTAGAGGTTCAGGGCAG-3′; Ard1ORFR1: 5′-CAACACGACACCTACAACGATGG-3′; DprF1: 5′-CGCCGTTCTTAAACTCAGTTCG-3′; DprSeqF1: 5′-GGAAAAAACGCCCTGCC-3′; DprSeqR1: 5′-GCACTTTCCCTCAACAC-3′; Ard1CloningR2: 5′-CATCAATAAAGTATGTTTACCGTTGGA-3′; DprSeqF2: 5′-CTCGCTAATTCAACCAC-3′; DprSeqR2: 5′-GTCTTTGCTTGCACTTG-3′; DprSeqF3: 5′-GAAGCGGGAGAAAGCTC-3′; Dpr61493R: 5′-CCCGAGAAATTGTTGGCG-3′; CG34356F3: 5′-CAACACAATCAACACAAGAACACG-3′.

Transgenic rescue

A genomic rescue construct was generated by amplifying a 3102 bp fragment encompassing the *Ard1* transcribed region and 1.3 Kb of flanking sequence from wild type genomic DNA using primers *Ard1 cloning F* (5′-CACCCGTTTGGCTGAAAATTCCTGC-3′) and *Ard1 cloning R2* (5-′CATCAATAAAGTATGTTTACCGTTGGA-3′). The PCR product was cloned into the Gateway™ entry vector pENTRD. After sequence verification the insert was transferred to pUASTattB-HW, a transformation vector containing φC31 *attB* sites and a Gateway™ destination vector cassette (Turan and Warrior, unpublished). Transgenic lines were recovered with the *Ard1* rescue construct inserted on the X and second chromosomes at the φX-2A and φX-22A sites (Bischof et al., 2007).

Quantitative PCR

Total RNA (2 μg) isolated from ovaries or female carcasses (RNeasy Mini Kit, Qiagen, Inc.) was used as substrate in a 20 μl reverse transcription reaction with an oligo(dT)16 primer (Omniscript Kit, Qiagen, Inc.). The first-strand cDNA (200 ng) served as template for quantitative RT-PCR performed with a DNA Engine Opticon™ continuous fluorescence detection system (MJ Research, Inc.). Each Q-PCR was performed four times using two independent biological samples. PCR specificity was confirmed by monitoring PCR product size and by melting curve analysis at each data point. The mRNA copy numbers for *Ard1* were standardized against *rp49* mRNA in each sample. Replicates from the same biological samples were first averaged for ΔCt calculation ($\Delta Ct = Ct_{wt} - Ct_{mt}$; C, cycle; t, threshold). Fold differences in *Ard1* transcript levels were calculated as $2^{\Delta Ct}$. Standard deviations were further derived from two averaged fold differences. Primers were as follows: *Ard1*: Forward 5′ TAGCGGTCAAGCGTTCCTATCG 3′ Reverse 5′-TTGGTGTAGAGGTTCAGGGCAG-3′; Rp49: Forward 5′-AGCGCACCAAGCACTTCATC-3′ Reverse 5′-GACGCACTCTGTTGTCGATACC-3′.

Generation of somatic clones

The vnc^{BDk} allele was used to generate vnc^{BDk} FRT-2A lines by recombination. Imaginal disc clones were generated by crossing vnc^{BDk} FRT-2A male flies to females homozygous for *hs*>FLP; *2xUbi-GFPnls* FRT-2A. Progeny were heat-shocked for 2 hours at 37°C for 3 consecutive days and reared at room temperature until dissection.

Immunohistochemistry and western blotting

Ovaries were dissected, fixed, and stained as described previously (Lei and Warrior, 2000). Antibodies used: mouse anti-ORB (1:50; 4H8; Developmental Studies Hybridoma Bank), mouse anti-Lamin (1:50; ADL67.10; DSHB), mouse anti-C(3)G (1:500; 1A8-1G2; gift from

R.S. Hawley), rabbit anti-C(3)G (1:3000; gift from M.A. Lilly), Rhodamine-Phalloidin (1:50; Molecular Probes), Alexa 488 goat anti-mouse (1:500; Molecular Probes), and DAPI (1:2000). The hybridomas 4H8, ADL67.10, 1B1 and JLA20 developed by P. Schedl, P. A. Fisher, H. D. Lipshitz and J. J-C Lin respectively were obtained from the Developmental Studies Hybridoma Bank developed under the auspices of the NICHD and maintained by The University of Iowa, Department of Biology, Iowa City. All images were acquired on Zeiss LSM510-META NLO confocal microscope and processed with Adobe Photoshop 7.0. Images were taken in Z-sections and projected as needed. Western blots were performed as previously described (Duncan and Warrior, 2002), with rabbit anti-human ARD1 (1:300; sc-33820; Santa Cruz Biotechnology), mouse anti-Actin (1:1,000; JLA20; DSHB) and HRP-conjugated goat anti-rabbit or anti-mouse secondary antibodies (1: 10,000; Jackson ImmunoResearch).

Supplementary Material

Refer to Web version on PubMed Central for supplementary material.

Acknowledgments

We thank Mary Lilly and Scott Hawley for sharing reagents and Mary Lilly for advice. We are especially grateful to Kavita Arora for constructive criticism and helpful insights.

Grant Sponsor: National Institutes of Health, NIGMS

Grant numbers: GM-71476 and GM-067247.

REFERENCES

Arnesen T, Anderson D, Baldersheim C, Lanotte M, Varhaug JE, Lillehaug JR. Identification and characterization of the human ARD1-NATH protein acetyltransferase complex. Biochem J 2005;386:433–443. [PubMed: 15496142]

Arnesen T, Gromyko D, Pendino F, Ryningen A, Varhaug JE, Lillehaug JR. Induction of apoptosis in human cells by RNAi-mediated knockdown of hARD1 and NATH, components of the protein N-alpha-acetyltransferase complex. Oncogene 2006;25:4350–4360. [PubMed: 16518407]

Arnesen T, Thompson PR, Varhaug JE, Lillehaug JR. The protein acetyltransferase ARD1: a novel cancer drug target? Curr Cancer Drug Targets 2008;8:545–553. [PubMed: 18991565]

Arnesen T, Van Damme P, Polevoda B, Helsens K, Evjenth R, Colaert N, Varhaug JE, Vandekerckhove J, Lillehaug JR, Sherman F, Gevaert K. Proteomics analyses reveal the evolutionary conservation and divergence of N-terminal acetyltransferases from yeast and humans. Proc Natl Acad Sci U S A 2009;106:8157–8162. [PubMed: 19420222]

Bischof J, Maeda RK, Hediger M, Karch F, Basler K. An optimized transgenesis system for Drosophila using germ-line-specific phiC31 integrases. Proc Natl Acad Sci U S A 2007;104:3312–3317. [PubMed: 17360644]

Chelsky D, Ralph R, Jonak G. Sequence requirements for synthetic peptide-mediated translocation to the nucleus. Mol Cell Biol 1989;9:2487–2492. [PubMed: 2668735]

Chintapalli VR, Wang J, Dow JA. Using FlyAtlas to identify better Drosophila melanogaster models of human disease. Nat Genet 2007;39:715–720. [PubMed: 17534367]

Clarke A, Orr-Weaver TL. Sister chromatid cohesion at the centromere: confrontation between kinases and phosphatases? Dev Cell 2006;10:544–547. [PubMed: 16678770]

Cooley L, Theurkauf WE. Cytoskeletal functions during Drosophila oogenesis. Science 1994;266:590–596. [PubMed: 7939713]

de Cuevas M, Lee JK, Spradling AC. alpha-spectrin is required for germline cell division and differentiation in the Drosophila ovary. Development 1996;122:3959–3968. [PubMed: 9012516]

de Cuevas M, Lilly MA, Spradling AC. Germline cyst formation in Drosophila. Annu Rev Genet 1997;31:405–428. [PubMed: 9442902]

de Cuevas M, Spradling AC. Morphogenesis of the Drosophila fusome and its implications for oocyte specification. Development 1998;125:2781–2789. [PubMed: 9655801]

Dej KJ, Spradling AC. The endocycle controls nurse cell polytene chromosome structure during Drosophila oogenesis. Development 1999;126:293–303. [PubMed: 9847243]

Deng W, Lin H. Spectrosomes and fusomes anchor mitotic spindles during asymmetric germ cell divisions and facilitate the formation of a polarized microtubule array for oocyte specification in Drosophila. Dev Biol 1997;189:79–94. [PubMed: 9281339]

Duncan JE, Warrior R. The cytoplasmic dynein and kinesin motors have interdependent roles in patterning the Drosophila oocyte. Curr Biol 2002;12:1982–1991. [PubMed: 12477386]

Evjenth R, Hole K, Karlsen OA, Ziegler M, Arnesen T, Lillehaug JR. Human Naa50p (Nat5/San) displays both protein N alpha- and N epsilon-acetyltransferase activity. J Biol Chem 2009;284:31122–31129. [PubMed: 19744929]

Fisher TS, Etages SD, Hayes L, Crimin K, Li B. Analysis of ARD1 function in hypoxia response using retroviral RNA interference. J Biol Chem 2005;280:17749–17757. [PubMed: 15755738]

Gautschi M, Just S, Mun A, Ross S, Rucknagel P, Dubaquie Y, Ehrenhofer-Murray A, Rospert S. The yeast N(alpha)-acetyltransferase NatA is quantitatively anchored to the ribosome and interacts with nascent polypeptides. Mol Cell Biol 2003;23:7403–7414. [PubMed: 14517307]

Goetze S, Qeli E, Mosimann C, Staes A, Gerrits B, Roschitzki B, Mohanty S, Niederer EM, Laczko E, Timmerman E, Lange V, Hafen E, Aebersold R, Vandekerckhove J, Basler K, Ahrens CH, Gevaert K, Brunner E. Identification and functional characterization of N-terminally acetylated proteins in Drosophila melanogaster. PLoS Biol 2009;7:e1000236. [PubMed: 19885390]

Goodrich JS, Clouse KN, Schupbach T. Hrb27C, Sqd and Otu cooperatively regulate gurken RNA localization and mediate nurse cell chromosome dispersion in Drosophila oogenesis. Development 2004;131:1949–1958. [PubMed: 15056611]

Hammond MP, Laird CD. Chromosome structure and DNA replication in nurse and follicle cells of Drosophila melanogaster. Chromosoma 1985;91:267–278. [PubMed: 3920017]

Hawkins NC, Thorpe J, Schupbach T. Encore, a gene required for the regulation of germ line mitosis and oocyte differentiation during Drosophila oogenesis. Development 1996;122:281–290. [PubMed: 8565840]

Hayden CA, Bosco G. Comparative genomic analysis of novel conserved peptide upstream open reading frames in Drosophila melanogaster and other dipteran species. BMC Genomics 2008;9:61. [PubMed: 18237443]

Horne-Badovinac S, Bilder D. Mass transit: epithelial morphogenesis in the Drosophila egg chamber. Dev Dyn 2005;232:559–574. [PubMed: 15704134]

Hou F, Chu CW, Kong X, Yokomori K, Zou H. The acetyltransferase activity of San stabilizes the mitotic cohesin at the centromeres in a shugoshin-independent manner. J Cell Biol 2007;177:587–597. [PubMed: 17502424]

Huynh, JR. Fusome as a cell-cell communication channel. In: Baluška, F.; Volkmann, D.; Barlow, PW., editors. Cell-Cell Channels. Springer; New York: 2006. p. 217-234.

Huynh JR, Johnston D. The role of BicD, Egl, Orb and the microtubules in the restriction of meiosis to the Drosophila oocyte. Development 2000;127:2785–2794. [PubMed: 10851125]

Jeong JW, Bae MK, Ahn MY, Kim SH, Sohn TK, Bae MH, Yoo MA, Song EJ, Lee KJ, Kim KW. Regulation and destabilization of HIF-1alpha by ARD1-mediated acetylation. Cell 2002;111:709–720. [PubMed: 12464182]

Kardon JR, Vale RD. Regulators of the cytoplasmic dynein motor. Nat Rev Mol Cell Biol 2009;10:854–865. [PubMed: 19935668]

Kashevsky H, Wallace JA, Reed BH, Lai C, Hayashi-Hagihara A, Orr-Weaver TL. The anaphase promoting complex/cyclosome is required during development for modified cell cycles. Proc Natl Acad Sci U S A 2002;99:11217–11222. [PubMed: 12169670]

King, RC. Ovarian Development in *Drosophila melanogaster*. Academic Press; New York: 1970.

Klattenhoff C, Xi H, Li C, Lee S, Xu J, Khurana JS, Zhang F, Schultz N, Koppetsch BS, Nowosielska A, Seitz H, Zamore PD, Weng Z, Theurkauf WE. The Drosophila HP1 homolog Rhino is required for transposon silencing and piRNA production by dual-strand clusters. Cell 2009;138:1137–1149. [PubMed: 19732946]

Kuo HP, Hung MC. Arrest-defective-1 protein (ARD1): tumor suppressor or oncoprotein? Am J Transl Res 2010;2:56–64. [PubMed: 20182582]

Kuo HP, Lee DF, Chen CT, Liu M, Chou CK, Lee HJ, Du Y, Xie X, Wei Y, Xia W, Weihua Z, Yang JY, Yen CJ, Huang TH, Tan M, Xing G, Zhao Y, Lin CH, Tsai SF, Fidler IJ, Hung MC. ARD1 stabilization of TSC2 suppresses tumorigenesis through the mTOR signaling pathway. Sci Signal 2010;3:ra9. [PubMed: 20145209]

Lantz V, Chang JS, Horabin JI, Bopp D, Schedl P. The Drosophila orb RNA-binding protein is required for the formation of the egg chamber and establishment of polarity. Genes Dev 1994;8:598–613. [PubMed: 7523244]

Lee L, Davies SE, Liu JL. The spinal muscular atrophy protein SMN affects Drosophila germline nuclear organization through the U body-P body pathway. Dev Biol 2009;332:142–155. [PubMed: 19464282]

Lei Y, Warrior R. The Drosophila Lissencephaly1 (DLis1) gene is required for nuclear migration. Dev Biol 2000;226:57–72. [PubMed: 10993674]

Leicht BG, Bonner JJ. Genetic analysis of chromosomal region 67A-D of Drosophila melanogaster. Genetics 1988;119:579–593. [PubMed: 3136051]

Lilly MA, de Cuevas M, Spradling AC. Cyclin A associates with the fusome during germline cyst formation in the Drosophila ovary. Dev Biol 2000;218:53–63. [PubMed: 10644410]

Lilly MA, Spradling AC. The Drosophila endocycle is controlled by Cyclin E and lacks a checkpoint ensuring S-phase completion. Genes Dev 1996;10:2514–2526. [PubMed: 8843202]

Lim JH, Park JW, Chun YS. Human arrest defective 1 acetylates and activates beta-catenin, promoting lung cancer cell proliferation. Cancer Res 2006;66:10677–10682. [PubMed: 17108104]

Lin H, Spradling AC. Fusome asymmetry and oocyte determination in Drosophila. Dev Genet 1995;16:6–12. [PubMed: 7758245]

Lin H, Yue L, Spradling AC. The Drosophila fusome, a germline-specific organelle, contains membrane skeletal proteins and functions in cyst formation. Development 1994;120:947–956. [PubMed: 7600970]

Liu Z, Xie T, Steward R. Lis1, the Drosophila homolog of a human lissencephaly disease gene, is required for germline cell division and oocyte differentiation. Development 1999;126:4477–4488. [PubMed: 10498683]

Mahowald, AP.; Kambysellis, MP. Oogenesis. In: Ashburner, M., editor. The Genetics and Biology of Drosophila. Academic Press; New York: 1980. p. 141-224.

Mathe E, Inoue YH, Palframan W, Brown G, Glover DM. Orbit/Mast, the CLASP orthologue of Drosophila, is required for asymmetric stem cell and cystocyte divisions and development of the polarised microtubule network that interconnects oocyte and nurse cells during oogenesis. Development 2003;130:901–915. [PubMed: 12538517]

Matthews KA, Rees D, Kaufman TC. A functionally specialized alpha-tubulin is required for oocyte meiosis and cleavage mitoses in Drosophila. Development 1993;117:977–991. [PubMed: 8325246]

McGrail M, Hays TS. The microtubule motor cytoplasmic dynein is required for spindle orientation during germline cell divisions and oocyte differentiation in Drosophila. Development 1997;124:2409–2419. [PubMed: 9199367]

McKearin D. The Drosophila fusome, organelle biogenesis and germ cell differentiation: if you build it. Bioessays 1997;19:147–152. [PubMed: 9046244]

McKearin D, Ohlstein B. A role for the Drosophila bag-of-marbles protein in the differentiation of cystoblasts from germline stem cells. Development 1995;121:2937–2947. [PubMed: 7555720]

Morris JZ, Hong A, Lilly MA, Lehmann R. twin, a CCR4 homolog, regulates cyclin poly(A) tail length to permit Drosophila oogenesis. Development 2005;132:1165–1174. [PubMed: 15703281]

Mullen JR, Kayne PS, Moerschell RP, Tsunasawa S, Gribskov M, Colavito-Shepanski M, Grunstein M, Sherman F, Sternglanz R. Identification and characterization of genes and mutants for an N-terminal acetyltransferase from yeast. Embo J 1989;8:2067–2075. [PubMed: 2551674]

Neuman-Silberberg FS. Drosophila female sterile mutation spoonbill interferes with multiple pathways in oogenesis. Genesis 2007;45:369–381. [PubMed: 17492752]

Ohlmeyer JT, Schupbach T. Encore facilitates SCF-Ubiquitin-proteasome-dependent proteolysis during Drosophila oogenesis. Development 2003;130:6339–6349. [PubMed: 14623823]

Page SL, Hawley RS. c(3)G encodes a Drosophila synaptonemal complex protein. Genes Dev 2001;15:3130–3143. [PubMed: 11731477]

Park EC, Szostak JW. ARD1 and NAT1 proteins form a complex that has N-terminal acetyltransferase activity. Embo J 1992;11:2087–2093. [PubMed: 1600941]

Pimenta-Marques A, Tostoes R, Marty T, Barbosa V, Lehmann R, Martinho RG. Differential requirements of a mitotic acetyltransferase in somatic and germ line cells. Dev Biol 2008;323:197–206. [PubMed: 18801358]

Polevoda B, Arnesen T, Sherman F. A synopsis of eukaryotic Nalpha-terminal acetyltransferases: nomenclature, subunits and substrates. BMC Proc 2009;3(Suppl 6):S2. [PubMed: 19660095]

Polevoda B, Sherman F. Composition and function of the eukaryotic N-terminal acetyltransferase subunits. Biochem Biophys Res Commun 2003a;308:1–11. [PubMed: 12890471]

Polevoda B, Sherman F. N-terminal acetyltransferases and sequence requirements for N-terminal acetylation of eukaryotic proteins. J Mol Biol 2003b;325:595–622. [PubMed: 12507466]

Reed BH, Orr-Weaver TL. The Drosophila gene morula inhibits mitotic functions in the endo cell cycle and the mitotic cell cycle. Development 1997;124:3543–3553. [PubMed: 9342047]

Rees, DM. Biology. Vol. vi. Indiana University; Bloomington, Indiana: 1990. A genetic and developmental analysis of mutations in alpha-Tub67C: a highly divergent, maternally expressed alpha-tubulin in Drosophila melanogaster; p. 223

Roth S, Jordan P, Karess R. Binuclear Drosophila oocytes: consequences and implications for dorsal-ventral patterning in oogenesis and embryogenesis. Development 1999;126:927–934. [PubMed: 9927594]

Schultz J, Pils B. Prediction of structure and functional residues for O-GlcNAcase, a divergent homologue of acetyltransferases. FEBS Lett 2002;529:179–182. [PubMed: 12372596]

Snapp EL, Iida T, Frescas D, Lippincott-Schwartz J, Lilly MA. The fusome mediates intercellular endoplasmic reticulum connectivity in Drosophila ovarian cysts. Mol Biol Cell 2004;15:4512–4521. [PubMed: 15292454]

Spradling, AC. Developmental genetics of oogenesis. In: Bate, M.; Martinez Arias, A., editors. *Drosophila* Development. Cold Spring Harbor Laboratory Press; Cold Spring Harbor, NY: 1993. p. 1-70.

Swan A, Nguyen T, Suter B. Drosophila Lissencephaly-1 functions with Bic-D and dynein in oocyte determination and nuclear positioning. Nat Cell Biol 1999;1:444–449. [PubMed: 10559989]

Van Buskirk C, Schupbach T. Half pint regulates alternative splice site selection in Drosophila. Dev Cell 2002;2:343–353. [PubMed: 11879639]

Volpe AM, Horowitz H, Grafer CM, Jackson SM, Berg CA. Drosophila rhino encodes a female-specific chromo-domain protein that affects chromosome structure and egg polarity. Genetics 2001;159:1117–1134. [PubMed: 11729157]

Williams BC, Garrett-Engele CM, Li Z, Williams EV, Rosenman ED, Goldberg ML. Two putative acetyltransferases, san and deco, are required for establishing sister chromatid cohesion in Drosophila. Curr Biol 2003;13:2025–2036. [PubMed: 14653991]

Yue L, Spradling AC. hu-li tai shao, a gene required for ring canal formation during Drosophila oogenesis, encodes a homolog of adducin. Genes Dev 1992;6:2443–2454. [PubMed: 1340461]

Zaccai M, Lipshitz HD. Differential distributions of two adducin-like protein isoforms in the Drosophila ovary and early embryo. Zygote 1996;4:159–166. [PubMed: 8913030]

Zhai RG, Hiesinger PR, Koh TW, Verstreken P, Schulze KL, Cao Y, Jafar-Nejad H, Norga KK, Pan H, Bayat V, Greenbaum MP, Bellen HJ. Mapping Drosophila mutations with molecularly defined P element insertions. Proc Natl Acad Sci U S A 2003;100:10860–10865. [PubMed: 12960394]

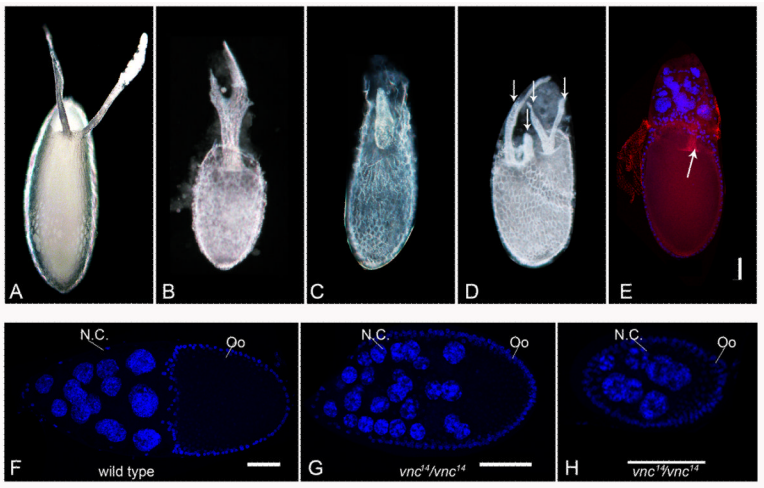

FIGURE 1. *vnc* mutants display chorion defects and variability in nurse cell number

Eggs (anterior upward) laid by wild type (A) and homozygous vnc^{14} or vnc^{14}/vnc^{BDk} females (B-D). (A) In wild type the paddle-like dorsal appendages (DA) arise from two distinct locations at the dorsal anterior region. (B) DAs are fused or more abnormally closely apposed in approximately 17% of eggs from *vnc* homozygotes. (C) More than 6% of eggshells are strongly ventralized with DAs reduced to a single structure. (D) Supernumerary DAs (arrows) are observed in ~1% of eggs. (E-H), Egg chambers stained with DAPI and rhodamine-phalloidin to detect nuclei (blue) and F-actin (red). (E) Nurse cells have failed to transfer their contents and the polyploid nuclei remain visible above the late stage *vnc* mutant egg chamber. Arrow marks the fused DAs. (F-H) Egg chambers oriented with anterior toward the left. (F) Wild type stage-10 egg chamber with 15 nurse cells (N.C., not all visible in this plane) and a single oocyte (Oo). By contrast, vnc^{14}/vnc^{14} mutant egg chambers have variable nurse cell numbers, as exemplified by a stage 9 egg chamber (G) containing 30 nurse cells, and a stage 5 egg chamber (H) containing only seven nurse cells. Scale bar in F-H = 50 μm.

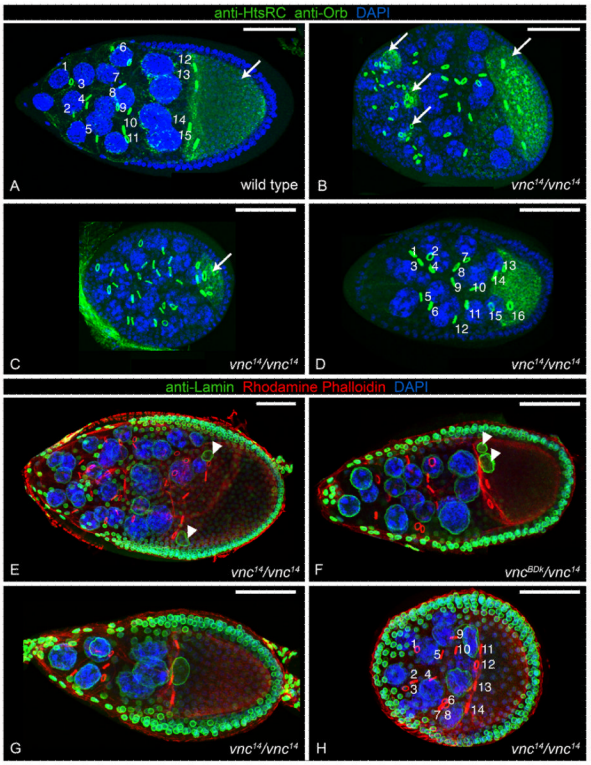

FIGURE 2. *vnc* mutant egg chambers contain abnormal numbers of germline cells

(A-D), Egg chambers stained with anti-ORB to identify the oocyte (diffuse cytoplasmic staining in green), anti-HTS-RC (also green) to show ring canals, and DAPI (blue) for DNA. (E-H), Egg chambers stained with anti-Lamin (ADL67.10; green) to mark the nuclear membrane, rhodamine phalloidin (red) for F-actin, and DAPI (blue) for DNA. (A) A wild type stage-9 egg chamber with 15 ring canals (numbered) and one oocyte (arrow). By contrast, in *vnc* mutant egg chambers (B-H) the nurse cell and ring canal numbers vary (60 nurse cells in B, 30 nurse cells in C, 16 nurse cells in D, and only 7 nurse cells in G). The presence of four oocytes in B (arrows) suggests an encapsulation defect, whereas association of five ring canals with the single oocyte (arrow) in C indicates that it has undergone an extra round of cell division. (E, F) Oocyte nuclear division is affected in *vnc* egg chambers. Lamin staining allows easy identification of the euploid oocyte nucleus. (E, F) Occasional mutant oocytes contain two nuclei (arrowheads) resulting from an additional nuclear division after oocyte specification or incomplete cytokinesis. (G) All germline cells have undergone only three divisions instead of four in this *vnc* egg chamber, yielding seven nurse cells and a single oocyte with three ring canals. (H) Egg chamber with 14 nurse cell nuclei and a single oocyte resulting from the failure of one nurse cell to divide. Scale bar = 50 μm.

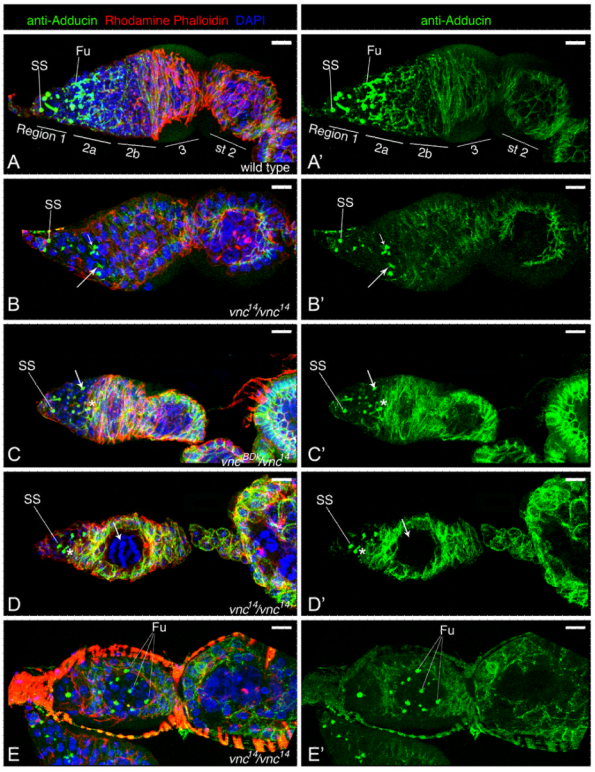

FIGURE 3. ***vnc*** **mutations perturb fusome morphology**

Germaria stained to visualize fusomes (anti-Adducin mAb1B1; green), filamentous actin (phalloidin; red) and DNA (DAPI; blue). (A, A′) Wild type germarium showing spectrosomes (SS) that give rise to highly branched fusomes (Fu), which maintain interconnections through the ring canals of daughter cystocytes as they divide. In *vnc* mutant germaria, spectrosomes appear largely unaffected but fusome morphology is highly variable, ranging from nearly wild type to reduced (long arrow) and fragmented (short arrow) (B, B′). (C, C′) Germaria in vnc^{14}/vnc^{BDk} females contain fewer fusomes that are less branched and assume spherical (arrow) or barbell shapes (asterisk). (D, D′) A severely affected vnc^{14} homozygous germarium contains few mostly unbranched fusomes. Only a single nurse cell (arrow) is present in the solitary stage 1 egg chamber. (E, E′) Occasionally fusome material is seen in the posterior of the germarium that contains more mature cysts, suggesting abnormal perdurance. Scale bar = 10 μm.

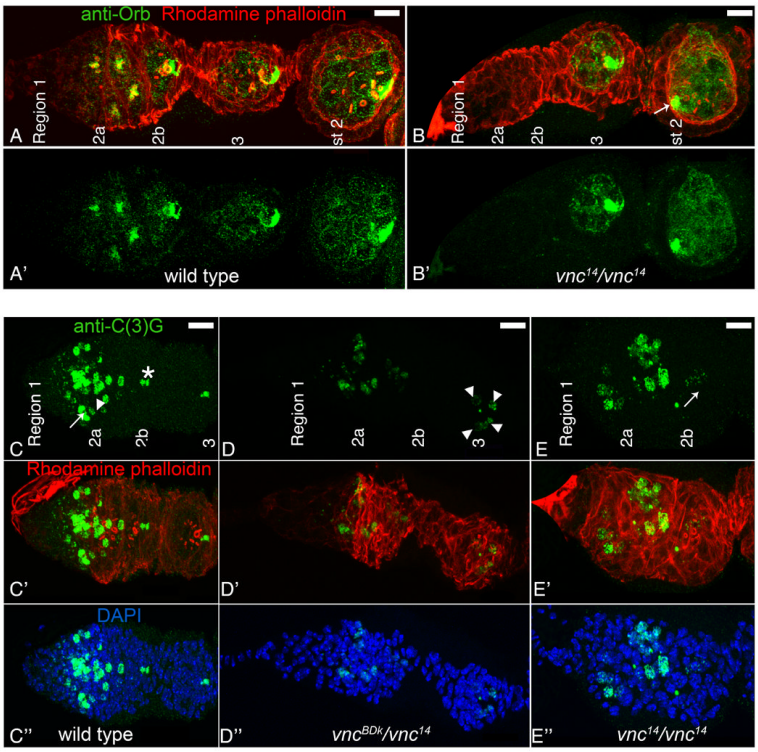

FIGURE 4. A subset of *vnc* mutant cysts show delayed oocyte specification

(A-B) Germaria and egg chambers stained to identify oocytes (anti-ORB; green) and actin (phalloidin; red). (A) ORB protein initially accumulates in two cystocytes in region 2a of a wild type germarium, but is restricted to a single cystocyte by late region 2a or early region 2b. (B) In a subset of vnc^{14} germaria, ORB is undetectable until region 3 where, as in wild type, it is present in a single cystocyte. Note that in the associated stage 2 egg chamber, the oocyte that stains with ORB (arrow) is mislocalized. (C-E) Germaria stained to visualize the synaptonemal complex (SC) component C(3)G (anti-C(3)G; green), F-actin (rhodamine-phalloidin; red) and DNA (DAPI; blue). (C) SC formation initiates in two to four cystocytes per 16-cell cyst in the multiple cysts present in region 2a of a wild type germarium. Punctate SC staining (arrowhead) is consistent with zygotene stage in meiotic prophase I, whereas continuous SC staining (arrow) is a hallmark of the pachytene stage. By the middle of region 2a, only two cystocytes per cyst retain SC staining, and by regions 2b and 3, only the oocyte retains SC staining (asterisks). (D) In a subset of vnc^{14}/vnc^{BDk} germaria, SC staining is seen in four germ line cells as late as germarial region 3, whereas in other samples (E), instead of becoming restricted to one cystocyte, SC staining is dispersed or is lost entirely by stage 2b. Scale bars = 10 μm.

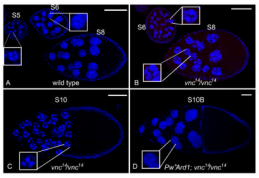

FIGURE 5. Nurse cell chromatin dispersal is delayed in *vnc* mutants

(A-D) Egg chambers stained with DAPI to visualize nuclei. Insets show magnified views of individual nuclei. (A) At stage 5 (S5), wild type nurse cell nuclei display a five-blob chromatin conformation wherein each blob corresponds to a major chromosome arm. During the transition to stage 6 (S6) the chromatin disperses more generally throughout the nucleus and the 5 blob conformation is lost. The chromatin remains dispersed throughout the remainder of egg chamber development (S8). In vnc^{14} homozygous ovaries the chromatin fails to disperse at stage 6 (B, S6) and retains the five-blob conformation through subsequent developmental stages (B, S8 and C, S10). (D) The chromatin dispersal defect in vnc^{14}mutant ovaries is completely rescued by a transgenic construct containing the ARD1 genomic region.

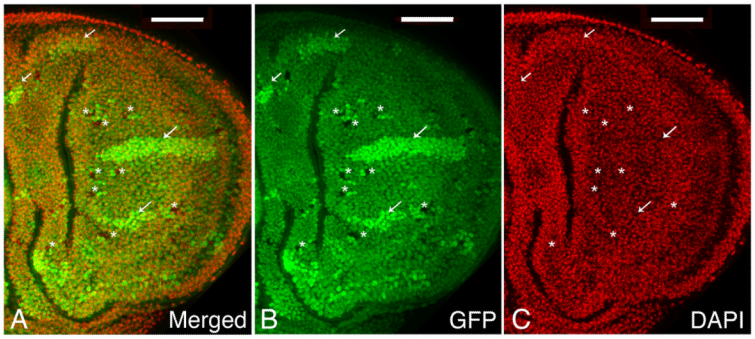

FIGURE 6. *vnc* affects cell proliferation or survival in wing discs

(A-C) Wing disc from a third instar vnc^{BDk} heterozygous larva subjected to multiple heat shocks to induce clones of homozygous mutant cells at different developmental stages. The presence of a GFP expressing transgene on the wild type chromosome enabled identification of mutant cells by the absence of GFP (asterisks). Nuclei (pseudocolored red) were marked by counterstaining with DAPI. Small clones of mutant cells can be detected that result from late induction of recombination. These clones that are adjacent to twin spots homozygous for GFP, were never observed to grow beyond four cells in size. No large mutant clones were detected despite the presence of large wild type twin spots resulting from early induction of recombination. Scale bar = 50 μm.

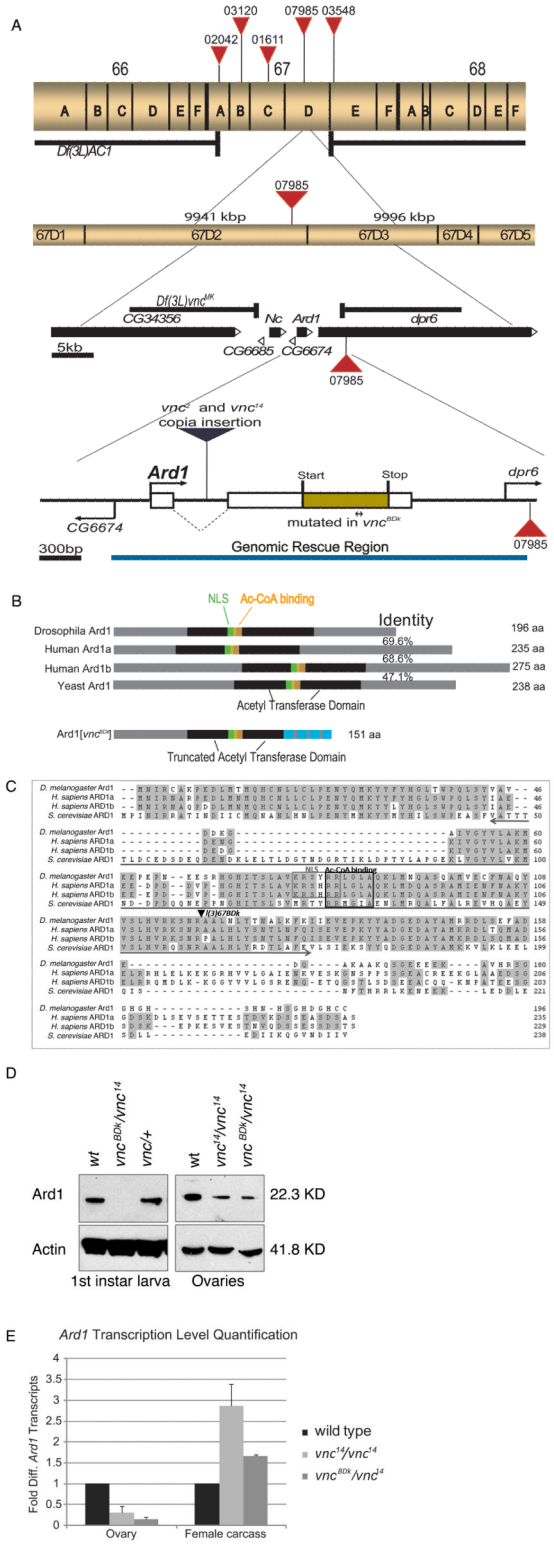

FIGURE 7. The *vnc* gene corresponds to the *Ard1* locus

(A) The cytogenetic region 66A-68F that contains the *Ard1* locus. The black bars bracket the extent of the deficiency *Df(3L)AC1* used to map the *vnc* locus. Red triangles mark the

insertion points of P-elements used in recombination mapping. The extent of deficiency *Df(3L)vnc*^{MK}, generated by imprecise excision of P-element 07985 is shown above the map of the genomic region surrounding *Ard1* (black bars indicate relative sizes of the indicated transcription units). The bottom of the panel depicts an expanded view of the *Ard1* locus including the transcription start site (bent arrow), 5′ and 3′ UTRs (open boxes) and the open reading frame (gold box). The copia insertion present in an identical position in the *Ard1* intron in both *vnc*^{2} and *vnc*^{14} is indicated by a black triangle. The blue bar indicates the extent of the genomic region used for successful transgenic rescue of the viability and sterility defects in *vnc* mutants. (B) Domain organization of ARD1 homologs. The acetyltransferase enzymatic domain is shown in black. The putative nuclear localization signal and the Ac-CoA binding motifs are shown in green and orange respectively. The extent of conservation of *Drosophila Ard1* (as compared with homologs in *S. cerevisiae* and *H. sapiens*) is also shown. The region affected in *vnc*^{BDk} that contains a frame-shift mutation in the acetyltransferase domain that truncates the enzymatic region is represented by the dashed blue bar. (C) Sequence alignment of *Drosophila*, human, and yeast ARD1 orthologs. Drosophila ARD1 protein shares 69.6% identity with human ARD1a and ARD1b (Ard2) and is 47.1% identical to yeast ARD1p. The acetyltransferase domain is indicated with a bi-directional arrow. The putative NLS and Ac-CoA binding motifs are enclosed in the grey and black boxes respectively. The arrowhead indicates the truncation start site in *vnc*^{BDk}. (D) Antibody against human ARD1 specifically recognizes the related *Drosophila* protein. Protein extracts from first instar larvae were western blotted and probed with anti-ARD1 antisera. A single band migrating at ~23 kDa was detected in extracts from wild type and *vnc* heterozygotes. No signal was detected in extracts from *vnc*^{BDk} hemizygotes demonstrating the specificity of the interaction. In ovary extracts ARD1 protein levels were reduced compared to wild type in both *vnc*^{14} homozygotes and *vnc*^{14}/*vnc*^{BDk} heterozygotes (D, right panels). Blots were re-probed with anti-actin antibodies as a loading control. (E) Real time PCR analysis indicates that compared to wild type *Ard1* transcript levels were reduced four-fold in ovaries from *vnc*^{14} homozygotes and eight-fold in *vnc*^{14}/*vnc*^{BDk} mutants. In female carcasses lacking ovaries *Ard1* transcript levels actually increased 2.86 fold in *vnc*^{14}/ *vnc*^{14} mutants and 1.5 fold in *vnc*^{14}/*vnc*^{BDk} mutants compared to wild type. *Ard1* transcript levels were normalized to *rp49*.

TABLE 1

Oogenesis defects in *vnc* mutant egg chambers

	Wild type		*vnc*^{14}/*vnc*^{14}		*vnc*^{14}/*vnc*^{BDk}		P{*w*$^{+}$ Ard1}; *vnc*^{14}/*vnc*^{14}		P{*w*$^{+}$ Ard1}; *vnc*^{14}/*vnc*^{BDk}	
Phenotype	**%**	**n**	**%**	**n**	**%**	**n**	**%**	**n**	**%**	**n**
Fusomes	0	59	46.7	120	28.3	60	3.9	103	3.8	79
C(3)G localization	3.1	98	12.8	78	13.2	38	3.6	112	5.9	51
Orb localization	0	95	10.5	86	11.4	35	1.4	70	3.1	65
Cystocyte division*	0	115	23.6	106	5.1	98	0.8	256	0.7	284
Cyst encapsulation	0.9	115	26.4	106	8.2	98	4.0	300	0.9	220
Chromatin dispersal	3.2	900	70.3	407	72.8	471	3.3	903	3.5	521
Dumpless	0	29	44.4	27	38.5	52	0	90	0	80
DA defect	1.5	200	24.6	244	28.2	110	4.4	180	3.3	150

Fusome and oocyte specification defects were scored in germaria while egg chambers were scored for defects in cystocyte division, cyst encapsulation, nurse cell chromatin dispersal (> stage 5) and dumping (> stage 11). DA defects were scored in embryos.

*Cystocyte division defects in *vnc*^{14} mutants include egg chambers with >15 (12.3%) and <15 nurse cells (11.3%).

TABLE 2

Recombination mapping of the *vnc* locus

P element	Molecular location (bp)	Total number of progeny scored	Number of w^- recombinants	Recombination distance (cM)
KG02042	9,294,869	4318	87	2.01
KG03120	9,456,099	4699	63	1.34
KG01611	9,766,952	5127	16	0.31
KG07985	9,968,287	6011	3	0.05
KG03548	10,331,071	5048	30	0.59